DETECTION OF NONLINEARITY IN A DYNAMIC SYSTEM USING DEFORMATION MODES OBTAINED FROM THE WAVELET TRANSFORM OF MEASURED RESPONSES

NGUYEN Viet Ha, PEETERS Maxime, GOLINVAL Jean-Claude

University of Liege,
Aerospace and Mechanical Engineering Department, Structural Dynamics Research Group
Chemin des Chevreuils 1, B52, B-4000 Liege, Belgium
Email : VH.Nguyen@doct.ulg.ac.be, M.Peeters@ulg.ac.be, JC.Golinval@.ulg.ac.be

SUMMARY: An efficient approach to Structural Health Monitoring of dynamical systems based on the Wavelet Transform (WT) and the concept of subspace angle is presented. The objective is to propose a detection method that is sensitive to the onset of nonlinear behaviour in a dynamic system. For this purpose, instantaneous frequencies are identified first from output-only vibration signals using the Wavelet Transform. Time varying deformation shapes are then extracted by analyzing the whole measurement data set on the structure. From this information, different dynamic states of the structure may be detected by inspecting time variations of 'modal' features. The experimental structure considered here as application example is a clamped beam with a geometric nonlinearity. Detection of nonlinearity is carried out by means of the concept of subspace angles between instantaneous deformation modes extracted from measurement data using the continuous Wavelet Transform. The method consists in controlling the angular coherence between active subspaces of the current and reference states respectively. The proposed technique, which shows a good sensitivity to small changes in the dynamic behaviour of the structure, may also be used for damage detection.

KEYWORDS: identification, nonlinearity, detection, subspace angle.

1. INTRODUCTION

Detection of changes in the dynamic state of structures is an important issue in the field of Structural Health Monitoring (SHM). It may be caused by the occurrence of damage but also by the onset of a nonlinear behaviour. Detection methods based on output-only vibration measurements attempt to extract features, which are sensitive to changes in the current dynamic state of the monitored structure.

Detection methods that use mathematical models include parametric and non-parametric techniques. Parametric methods require the construction of a structural model and are based on model updating techniques [1-3]. A precise model is of primary importance in this case; it offers the advantage to allow damage location and possibly remaining lifetime calculation but it generally needs a lot of modelling and computation time. Non-parametric methods do not require a structural model. They may be based on the direct use of modal parameters (natural frequencies and mode shapes), or stiffness and flexibility matrices. For example, some techniques are based on principal component analysis (PCA) of vibration measurements [4] or on a combination of independent component analysis (ICA) with neural networks [5]. However, most of the methods are based on the assumption of stationarity of the signals and lead to the identification of a unique set of 'modal' features. Time-frequency decompositions are helpful to capture transient dynamic features that appear during operation. One of them is the Hilbert-Huang transform (HHT) [6] that has been developed in the last decade to handle both identification and detection problem [7-8]. One of the main drawbacks of the HHT method relies in its empirical formulation. Conversely the theoretical basis of the Wavelet Transform (WT) makes it more appropriate for non-stationary data analysis. Gurley and Kareem [9] used both the continuous and discrete WT for identification and characterization of transient random processes. In parallel with other techniques of image processing, the discrete WT is utilized in [10] by Wang *et al.* to recognize the mode shapes of 2D structures. Using Morlet wavelet, Kijewski and Kareem [11] deal with system identification in civil engineering and Staszewski [12] with identification of systems with cubic stiffness nonlinearity. Argoul, Le and Erlicher [13-15] use the continuous Cauchy wavelet transform as a tool for modal identification in linear and nonlinear systems. In [13], four instantaneous indicators are proposed to facilitate the characterization of the nonlinear behaviour of a structure.

The aim of this paper is to propose an alternative method to detect nonlinearity using the Wavelet Transform and the concept of subspace angles. Morlet wavelet is considered here as the mother wavelet to extract instantaneous frequencies and amplitudes from time measurements at different locations on the structure. Deformation modes

associated to instantaneous frequencies may then be extracted from the whole data set and assembled to build instantaneous observation matrices Singular value decomposition of these matrices allows to determine the dimensionality of the system. Next, the retained deformation shapes are compared with reference mode-shapes using the concept of subspace angle. The objective is to provide an index able to detect the onset of the nonlinear behaviour of the structure. The proposed technique is illustrated on the example of a clamped beam, which exhibits a geometric nonlinearity at one end. It shows a good sensitivity to small changes in the dynamic behaviour of the structure and thus may also be used for damage detection.

2. WAVELET TRANSFORM (WT)

A wavelet is a zero mean function $\psi(t) \in \mathcal{L}^2(\Re)$, with unitary norm and centered in the neighborhood of $t = 0$. The functions $\psi_{u,s}(t)$ are obtained by dilating the mother wavelet by a scale factor s and translating it by u:

$$\psi_{u,s}(t) = \frac{1}{\sqrt{s}}\psi\left(\frac{t-u}{s}\right) \tag{1}$$

The wavelet transform consists in decomposing the signal $f(t) \in \mathcal{L}^2(\Re)$ into a series of basis wavelet functions through the convolution of the signal and the scaled mother wavelet according to:

$$Wf(u,s) = \frac{1}{\sqrt{s}}\int_{-\infty}^{+\infty} f(t)\bar{\psi}\left(\frac{t-u}{s}\right)dt \tag{2}$$

where $u,s \in \Re$ and the bar is used to denote the complex conjugate.
The function $\psi_{u,s}(t)$ is centered in the neighborhood of u. If $\hat{\psi}(\omega)$ presents the Fourier transform (FT) of $\psi(t)$ in $\mathcal{L}^2$, the central frequency of $\hat{\psi}(\omega)$ is ξ, then the central frequency of a dilated function is ξ / s. The wavelet coefficients, $Wf(u,s)$, designate the similitude between the dilated and translated mother wavelet and the signal at the time t and at the scale (frequency) s. Thanks to its ability to consider time and frequency resolutions at the same time, the WT is particularly well adapted to detect discontinuity or sharp signal transitions.
The function $\psi(t) \in \mathcal{L}^2$ must satisfy a condition, called *admissibility condition*, which allows to analyze the signal and then to reconstruct it without loss of information:

$$C_\psi = \int_0^{+\infty} \frac{|\hat{\psi}(\omega)|^2}{|\omega|}d\omega < +\infty \tag{3}$$

Moreover, the admissibility condition implicates that the FT of the wavelet must be zero at the frequency $\omega = 0$:

$$\hat{\psi}(\omega)\big|_{\omega=0} = 0 \tag{4}$$

It implies two important consequences: 1) the wavelets must have a band-pass spectrum; 2) the equivalence of the last equation under the form: $\int_{-\infty}^{+\infty} \psi(t)dt = 0$. This expression shows that $\psi(t)$ must be zero mean. $\psi(t)$ is thus a function of finite larger in time (time window) possessing an oscillation characteristic.
The WT has a time frequency resolution, which depends on the scale s. The time spread is proportional to s while the frequency spread is proportional to the inverse of s. In both time and frequency domains, the optimal resolutions are attained if and only if the wavelet function is Gaussian. Furthermore, the wavelet shows a good precision in frequency for a low frequency and a good precision in time for a high frequency.
Using the Parseval formula:

$$\int_{-\infty}^{+\infty} f(t)\bar{g}(t)dt = \frac{1}{2\pi}\int_{-\infty}^{+\infty} \hat{f}(\omega)\bar{\hat{g}}(\omega)d\omega,$$

the Wavelet Tranform can be computed by the Fourier transform:

$$Wf(u,s) = \frac{\sqrt{s}}{2\pi} \int_{-\infty}^{+\infty} \hat{f}(\omega)\bar{\hat{\psi}}(s\omega)e^{j\omega u} d\omega \tag{5}$$

For each scale *s*, one computes the inverse transform of the product of signal $f(t)$ and the dilated versions $\hat{\psi}(s\omega)$ of the mother wavelet $\psi(t)$. In numerical applications, the WT computation is completed practically through the fast Fourier transform (FFT) algorithm.
So, thanks to its ability to consider time and frequency resolutions at the same time, the WT is particularly well adapted to detect discontinuity or sharp signal transitions.

2.1 Choice of wavelet

To separate amplitude and phase information of signals, one uses analytic complex wavelets, which have the property of progressiveness, i.e. its Fourier transform $\hat{\psi}(\omega) = 0$ for $\omega < 0$. The progressiveness ensures the WT does not produce any interference between the past and future in the time domain. Many analytic wavelets are studied in the literature. The choice of mother wavelet depends on several analysis properties. For a time-frequency analysis, a wavelet for which the localization in time and in frequency is optimal is ideal. The Morlet wavelet is very popular in the literature because its analogues to the Fourier transform are useful for harmonic analysis. It is the reason why it is chosen in this work. The Morlet wavelet is defined by:

$$\psi_M(t) = g(t)e^{j\omega_0 t} \qquad \text{with} \qquad g(t) = 1/\sqrt[4]{\pi\sigma^2}.e^{-\frac{t^2}{2\sigma^2}} \tag{6}$$

where ω_0 is the central frequency of $\hat{\psi}$ and the parameter σ arranges time and frequency resolutions.
Dilatations of this temporally localized mother wavelet permit to discover harmonic components within the signal. The Morlet wavelet in (6) is a Gaussian-windowed Fourier transform, this window is optimal as it has the same resolution in both the time and frequency domains.
If $\sigma^2\omega_0^2 >> 1$, the Morlet wavelet is considered as approximately analytical with zero mean and admissible. For practical purposes, a high enough value of the product $\omega_0\sigma$ can be chosen such as $\omega_0\sigma \geq 5$. The FT of $\psi_M(t)$ reaches the maximum at $s\omega = \omega_0$ and it leads to a relation between instantaneous frequency and scale: $\omega = \omega_0 / s$.

2.2. Wavelet ridges

If $a(u)$ and $\phi(u)$ are respectively instantaneous amplitude and phase, the WT is also given by:

$$Wf(u,s) = \frac{\sqrt{s}}{2} a(u)e^{j\phi(u)} \left\{ \hat{g}\left[s\left(\omega - \phi'(u)\right)\right] + \varepsilon\left(u,\omega\right)\right\} \tag{7}$$

where $\varepsilon(u,\omega)$ is a corrective term [16]. If this term is negligible, it is clear that (7) enables to measure $a(u)$ and $\phi'(u)$ from $Wf(u,s)$. The corrective term is negligible if $a(u)$ and $\phi'(u)$ have small variations over the support of $\psi_{u,s}$ and $\phi'(u) \geq \Delta\omega / s$, that $\Delta\omega$ is bandwidth of $\hat{g}$.
Different methods exist to define and to extract ridges [12, 13 and 16]. The scalogram gives a time-frequency representation of the energy contained in the signal $f(t)$ in the neighbourhood of (u,ω). The normalized scalogram is defined by:

$$P_W^{norm} f\left(u,\omega\right) = \frac{1}{s}\left|Wf\left(u,s\right)\right|^2 \tag{8}$$

for $\omega = \frac{\omega_0}{s}$ where ω_0 is the central frequency of the mother wavelet.
The frequencies that correspond to the maximum of $|Wf(u,s)|$ constitute the ridge. Here, the ridge algorithm computes instantaneous frequencies from local maxima of the scalogram, corresponding to dominant frequency components in the signal at each time instant (Figure 1).
If $\Phi_W(u,\omega)$ is the complex phase of $Wf(u,s)$, at ridge points, the instantaneous frequency $\phi'(u)$ and the analytic amplitude $a(u)$ are given respectively by:

$$\phi'(u) = \omega = \frac{\partial \Phi_W(u,\omega)}{\partial u} \quad \text{and} \quad a(u) = \frac{2}{|\hat{g}(0)|}\sqrt{\frac{P_w^{norm} f(u,\omega)}{s}} \tag{9}$$

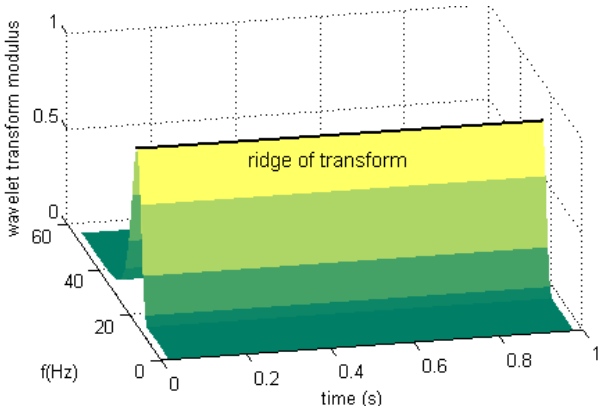

Figure 1 - Identification of instantaneous frequency using wavelet ridge for the signal $f(t) = e^{j\omega t}$

When $\omega = \phi'(u)$, the corrective term $\varepsilon(u,\omega)$ is negligible if:

$$\frac{\omega_0^2}{|\phi'(u)|^2}\frac{|a''(u)|}{|a(u)|} << 1 \quad \text{and} \quad \omega_0^2 \frac{|\phi''(u)|}{|\phi'(u)|^2} << 1 \tag{10}$$

The presence of ϕ' in the denominator shows that a' and ϕ' may vary slowly if ϕ' is small but may vary much faster for larger instantaneous frequencies.

2.3. Multiple frequencies

An important key in the analysis of multi-component signal is the choice of the mother wavelet parameters in order to discriminate each component. Let $\phi_1'(u)$ and $\phi_2'(u)$ be instantaneous frequencies of two different components, the ridges do not interfere if the dilated window gets sufficient frequency resolution at the ridge scales:

$$\hat{g}\left(s|\phi_1'(u) - \phi_2'(u)|\right) \approx 1 \tag{11}$$

Define $\Delta\omega$ as bandwidth of $\hat{g}(\omega)$ by: $\hat{g}(\omega) \approx 1$ for $|\omega| \geq \Delta\omega$. Expression (11) means that the wavelet needs an enough small value for $\Delta\omega/\omega_0$ in order to isolate those spectral components:

$$\frac{|\phi_1'(u) - \phi_2'(u)|}{\phi_1'(u)} \geq \frac{\Delta\omega}{\omega_0} \quad \text{and} \quad \frac{|\phi_1'(u) - \phi_2'(u)|}{\phi_2'(u)} \geq \frac{\Delta\omega}{\omega_0} \tag{12}$$

Parameter ω_0 of the mother wavelet must be chosen in an adequate manner to satisfy simultaneously the conditions (10) and (12). If two spectral lines are too close, they interfere so that the ridge pattern is destroyed. The spectral line number is generally unknown. Ridges corresponding to a low amplitude are often carried off because they may be due to noise, or correspond to "shadows" of other instantaneous frequencies created by the side-lobes of $\hat{g}(\omega)$.

3. DETECTION BASED ON THE CONCEPT OF SUBSPACE ANGLE

For a given excitation, the WT allows to identify the instantaneous frequencies (or ridges) at a set of different measurement coordinates on the structure. Accordingly, it provides the amplitude ratios between coordinates in each instantaneous deformation mode associated to an identified ridge line. Using these ratios, one can assess time-varying deformation ('mode') shapes of the system. The modes with the strongest energies may be

regarded as active modes and used to construct active subspaces at different time instants (or states of the system). A change in the dynamic behaviour modifies consequently the state of the system, i.e. the instantaneous frequencies and deformation shapes. This change may be estimated using the concept of subspace angle introduced by G.H. Golub and C.F. Van Loan [17]. This concept was used in [4] as a tool to quantify existing spatial coherence between two data sets resulting from observation of a vibration system. Given two subspaces (each with linear independent columns) $\mathbf{S} \in \Re^{n \times p}$ and $\mathbf{D} \in \Re^{n \times q}$ ($p>q$), the procedure is as follows. Carry out the QR factorizations: $\mathbf{S} = \mathbf{Q}_S\mathbf{R}_S$ ($\mathbf{Q}_S \in \Re^{n \times p}$) and $\mathbf{D} = \mathbf{Q}_D\mathbf{R}_D$ ($\mathbf{Q}_D \in \Re^{n \times q}$). The columns of $\mathbf{Q}_S$ and $\mathbf{Q}_D$ define the orthonormal bases for **S** and **D** respectively. The angles θ_i between the subspaces **S** and **D** are computed from singular values associated with the product $\mathbf{Q}_S^T\mathbf{Q}_D$:

$$\mathbf{Q}_S^T \mathbf{Q}_D = \mathbf{U}_{SD} \boldsymbol{\Sigma}_{SD} \mathbf{V}_{SD}^T \; ; \quad \boldsymbol{\Sigma}_{SD} = \mathrm{diag}\left(\cos\left(\theta_i\right)\right) \quad i = 1...q \tag{13}$$

The largest singular value is thus related with the largest angle characterizing the geometric difference between two subspaces.
The onset of nonlinearity in a structure may be detected by monitoring the angular coherence between subspaces estimated from the reference observation set and from the observation set of a current state respectively. A state is considered as a reference state if the system operates in normal condition (nonlinearity is not activated or damage does not exist).

4. WT APPLICATION TO DETECT NONLINEARITY

The example consists in identifying the modal features and in detecting the level of nonlinearity in a cubic stiffness system by means of the WT. The analysis is conducted both numerically and experimentally. The studied structure is a beam clamped at one end and exhibiting a cubic stiffness at the other end (Figure 2).

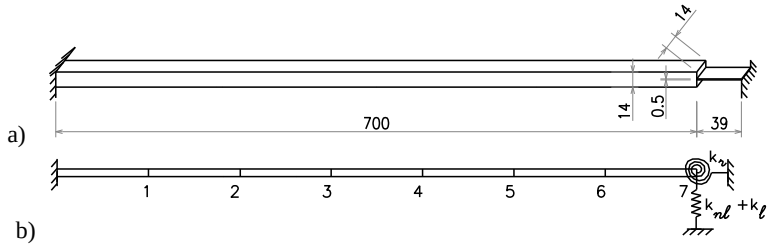

Figure 2 - The beam with a nonlinear stiffness (a) and its finite element model (b)

The cubic stiffness is realised by means of a very thin beam. For weak excitation, the system behaviour may be considered as linear. When the excitation level increases, the thin beam exhibits large displacements and a nonlinear geometric effect is activated resulting in a stiffening effect at the end of the main beam. The structure was used as a benchmark for nonlinear system identification during the European action COST F3 [13, 18].

4.1. Numerical analysis

The main beam is modelled with seven beam finite elements (Figure 2b). The thin beam is represented by two equivalent grounded springs: one in translation ($k_l + k_{nl}$) and one in rotation (k_r). The nonlinear stiffening effect of the thin beam is modelled by a nonlinear function in displacement of the form: $f_{nl}(x) = A|x|^{\alpha}\,\mathrm{sign}(x)$, where A is a nonlinear coefficient, $A = 6\times10^9\,N/m^3$ and α is a nonlinear exponent, $\alpha = 3$. These parameters were determined experimentally in reference [18].

Nonlinear normal modes

The nonlinear normal modes (NNMs) of this structure were calculated in reference [19]. These modal features depend on the total energy in the system as illustrated in Figure 3 by the frequency-energy plot (FEP) of the first and the second NNMs.

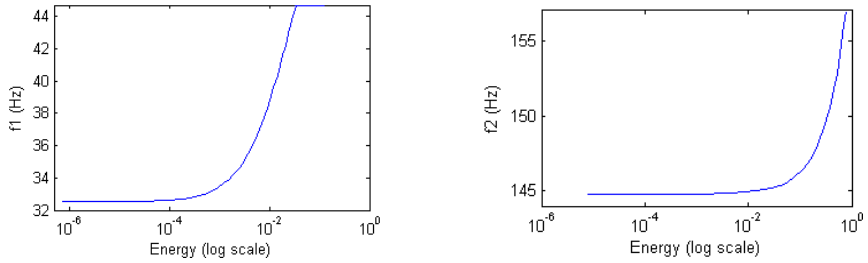

a) First NNM b) Second NNM

Figure 3 - Frequency-energy plot of the first (a) and second (b) NNMs

The first and second NNM motions are plotted in Figure 4 at low and high energy level respectively. The low energy level (actually the linear normal modes) corresponds to f_1 = 32.60 Hz and f_2 = 144.79 Hz while the high energy level (the nonlinear case) corresponds to f_1 = 38.46 Hz and f_2 = 147.67 Hz.

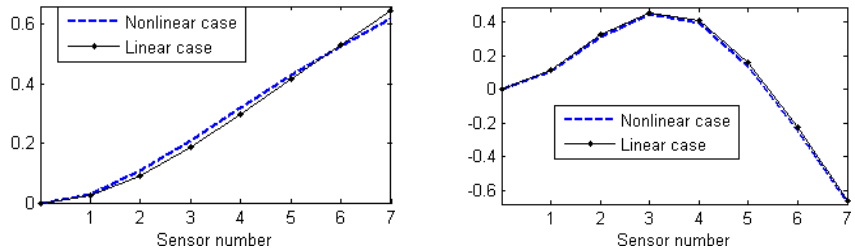

Figure 4 - Analytical deformation shapes of the 1st, 2nd modes respectively

Impact excitation

For the purpose of this study, the beam is supposed to be submitted to an impact force at its right end. The free response of the structure is measured in the vertical direction at the seven coordinates indicated in Figure 2b and the WT is applied to the measured data. Starting at a 'low' excitation level (impact of 70N), the behaviour of the beam appears as linear (the largest displacement is lower than 0.15 mm). The WT of the displacement at coordinate n°7 is given in Figure 5 in terms of instantaneous frequencies and amplitudes. Two frequency lines (called 'ridges') are observed respectively at 32.6 Hz and 144.7 Hz, which is in agreement with the frequencies occurring at low energy in the FEP (Figure 3). Higher frequencies of small amplitudes could also be detected [18] but they are not considered here.

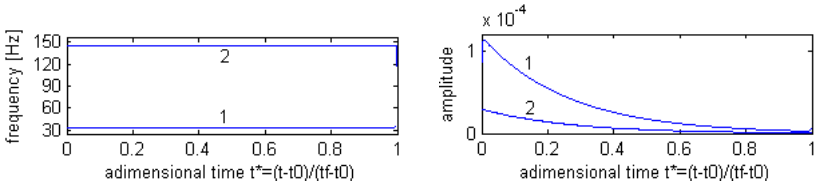

Figure 5 - Instantaneous frequencies and amplitudes at low energy (linear case)

Let us consider next a high level of excitation (impact of 1500N) corresponding to a maximum displacement at the right end of about 2.4 mm. Figure 6 presents the corresponding WT results. It clearly shows a drop-off of the frequencies down to the linear system values as the nonlinear effect vanishes progressively and the amplitude goes down. Figure 6 also reveals the presence of a 3 order super harmonic of the first frequency (curve n° 3).

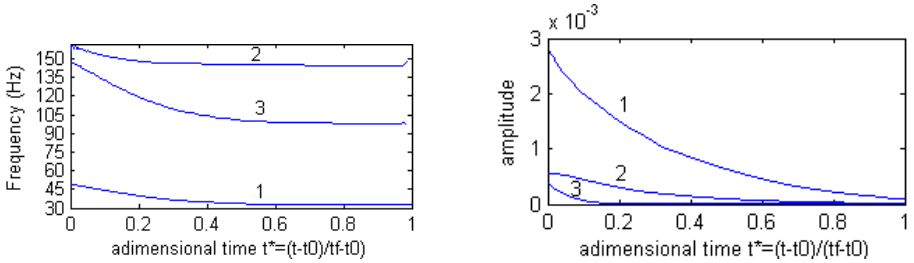

Figure 6 - Instantaneous frequencies and amplitudes at high energy (nonlinear case)

Identification of deformation shapes and detection of nonlinear behaviour

Figure 7 presents the first two modes of the beam identified with the 'low' impact excitation when the dynamic behaviour of the structure may be considered as linear.

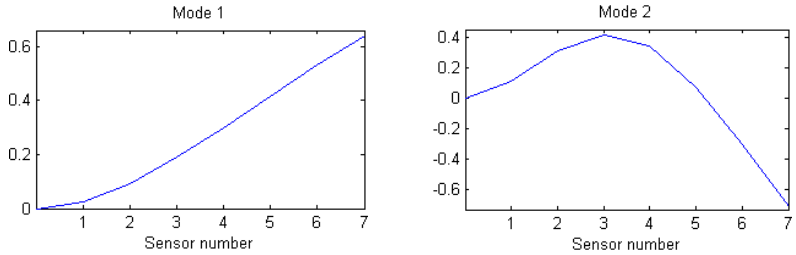

Figure 7 - Mode 1 and 2 in the linear case

Figure 8 gives the deformation shapes at higher excitation levels. When the displacement at the right end starts to be significant, both the first two deformation shapes associated to ridges n° 1 and n° 2 become influenced by the magnitude of the nonlinearity of the structure (the reference shape corresponds to the linear normal modes shown in Figure 7). For high excitation levels, a super harmonic of the first frequency appears as illustrated by the ridge line n° 3 in Figure 6. It is interesting to note that one can find an intermediate deformation shape from this ridge line; the last plot of Figure 8 gives the corresponding deformation shapes for different amplitudes of the displacement at the right end of the beam.

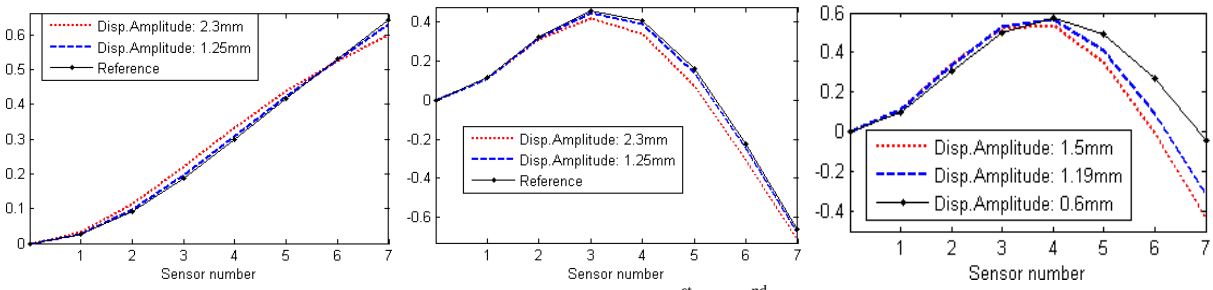

Figure 8 - Deformation shapes associated to the 1st, the 2nd and the super harmonic modes

The instantaneous deformation shapes $\mathbf{M}_1$, $\mathbf{M}_2$ and $\mathbf{M}_3$ corresponding to the three ridges allow defining an instantaneous deformation matrix $\mathbf{A} = [\mathbf{M}_1 \ \mathbf{M}_2 \ \mathbf{M}_3]$. Performing the singular-value decomposition (SVD) of matrix $\mathbf{A}$, it can be shown that the third (super harmonic) deformation mode ($\mathbf{M}_3$) is actually a linear combination of the two other modes. Figure 9 shows the instantaneous singular values of the decomposition in terms of energy percentage. It reveals that the third singular value is negligible compared to the two others.

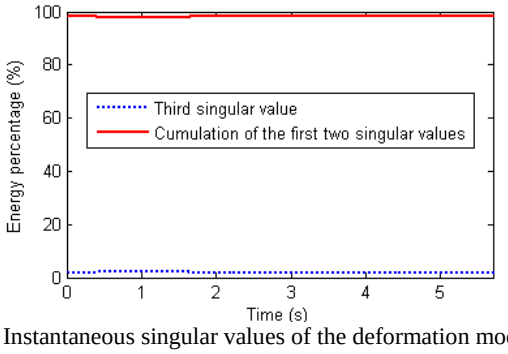

Figure 9 - Instantaneous singular values of the deformation mode matrix

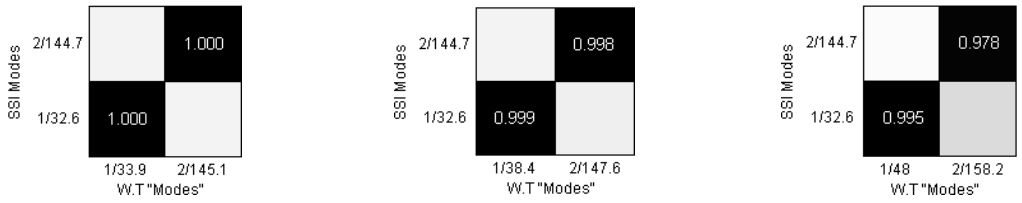

a) Displacement amplitude ≈ 0.6 mm b) Displacement amplitude ≈ 1.25 mm c) Displacement amplitude ≈ 2.3 mm

Figure 10 - MAC between WT and SSI modes

The comparisons may be equally carried out by means of the MAC (**M**odal **A**ssurance **C**riterion). In Figure 10, deformation modes obtained through the WT are compared with the linear normal modes identified by the SSI method (**S**tochastic **S**ubspace **I**dentification) for different values of the displacement at the end of the beam. When the displacement is low (Figure 10a), the MAC indicates a perfect correlation. At this level of excitation, the deformation shapes are identical to the linear normal modes. On the other hand, when the displacement amplitude is high (Figure 10c), the nonlinearity is well excited, which results in a frequency increase and a slight loss of correlation with the linear normal modes (identified by SSI). Figure 10 shows however that the MAC is not a deciding criterion for the detection of nonlinearity.

Detection based on the concept of subspace angle

For the purpose of detection of nonlinearity, the structure is now supposed to be excited at increasing level of impact force (amplitudes ranging from 100 N to 1500 N). The corresponding instantaneous frequencies obtained through the WT of the response signals at coordinate n°7 are shown in Figure 11.

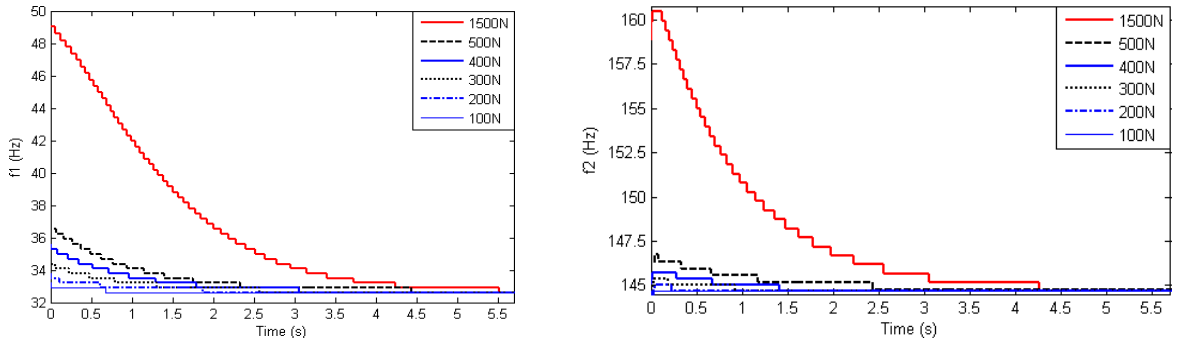

Figure 11 - Instantaneous frequencies corresponding to different excitation levels

As explained in section 3, the instantaneous deformation shapes associated to these two frequencies may be considered as instantaneous active modes to define a subspace, which characterises the dynamic state of the structure. The comparison of subspace angles between the reference state (defined by the linear normal modes) and current states at different excitation levels reveals the range of activation of the nonlinearity as illustrated in Figure 12. Larger is the excitation level, more significant is the angle. As responses are damped, the angles reach their largest values at the beginning and then decrease gradually to converge to zero as the dynamic behaviour of the beam becomes linear.

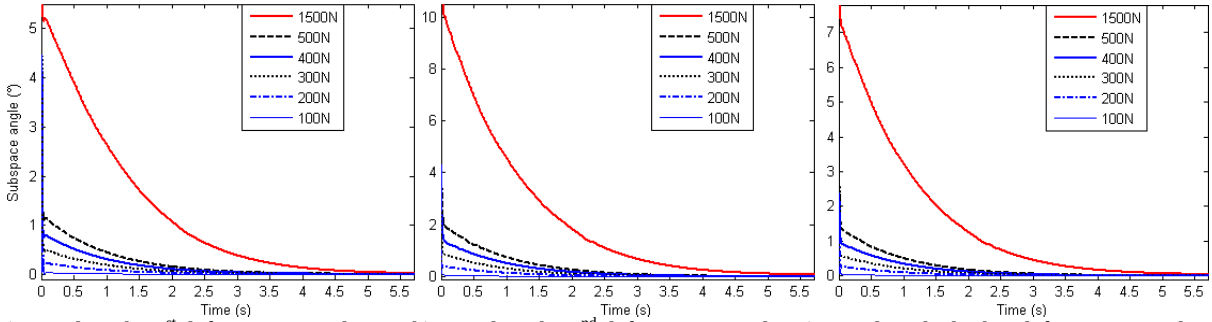

a) Based on the 1st deformation mode b) Based on the 2nd deformation mode c) Based on the both 2 deformation modes

Figure 12 - Time evolution of subspace angles for different excitation levels

As the activation of the nonlinearity depends on the amplitude level of the displacement, the display of subspace angles according to the evolution of the instantaneous displacement amplitude measured at the end of the beam is informative. Figure 13 shows the evolution of subspace angles in function of the displacement amplitude measured at the end of the beam at time t = 0.1 *s*. It can be observed that the subspace angle criterion for the 2nd mode is more sensitive to the nonlinearity in comparison to the 1st mode (which is confirmed by the MAC in Figure 10). In terms of frequency changes however, the 1st mode appears as more affected than the 2nd mode (Figure 11).
In summary, the onset of nonlinearity may be detected by observing the evolution of instantaneous frequencies as illustrated in Figure 11 but a high frequency resolution is needed to distinguish between close levels of excitation (e.g. impacts of 100 N to 500 N). In this respect, subspace angle curves look more promising as they look less affected by the frequency resolution. Another advantage is that the concept of subspace angle allows to handle several modes simultaneously in a unique detection index.

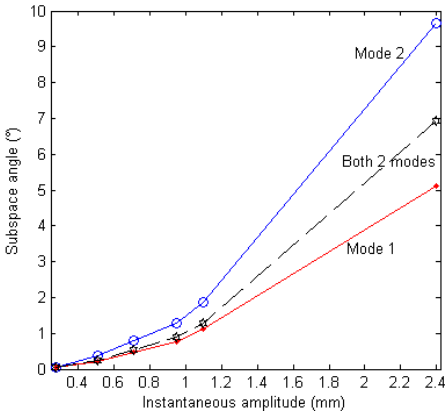

Figure 13 - Relation angle–displacement amplitude at the end of the beam at t = 0.1*s*

4.2. Experimental results
Experimental results were collected using 7 accelerometers located at the coordinates given in Figure 2.
An impact of very low amplitude was first applied at the end of the beam to obtain the reference state. The first two natural frequencies are observed at 31.3 Hz and 143.5 Hz respectively as shown in Figure 14, which gives the WT of the response measured at the end of the beam (coordinate n° 7). These values are slightly lower than the frequencies predicted by the numerical model, which is mainly due to the influence of the mass of the sensors.

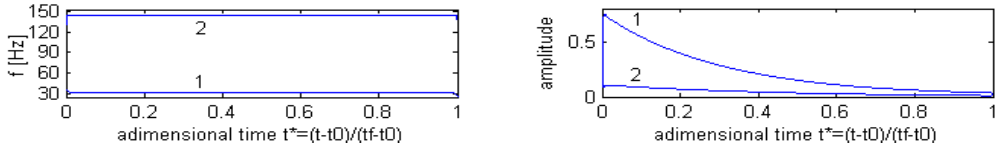

Figure 14- Instantaneous frequencies and amplitudes corresponding to an impact of low amplitude

An impact of higher amplitude was then applied to activate the nonlinearity. The results are shown in Figure 15. It is observed that three instantaneous frequencies (ridges) are detected and that they are decreasing in time.

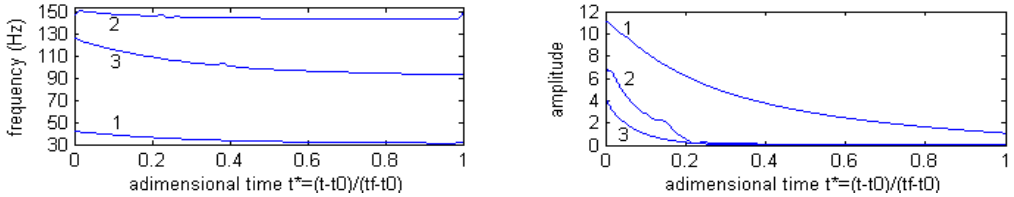

Figure 15 - Instantaneous frequencies and amplitudes when the nonlinearity is activated

The deformation modes corresponding to those three frequencies are presented in Figure 16 at different instants (corresponding to different levels of displacement at the end of the beam).

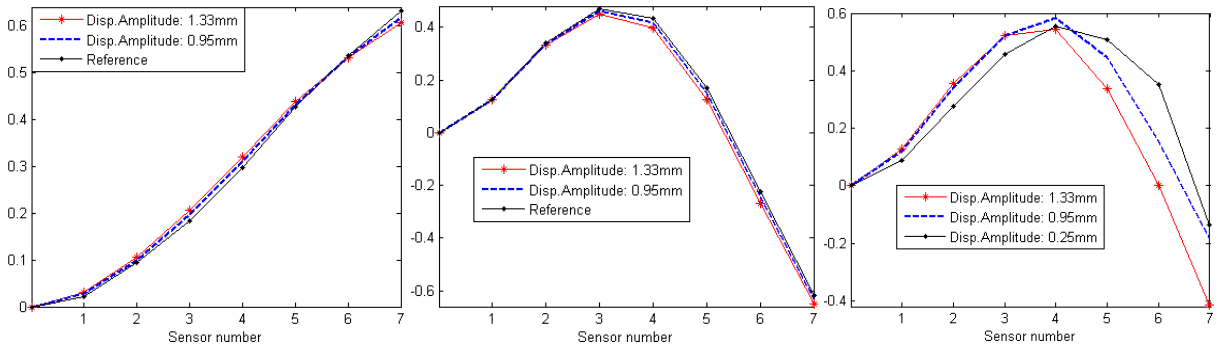

a) From the first frequency ridge b) From the second frequency ridge c) From the third frequency ridge

Figure 16 - Deformation modes corresponding to different displacement amplitudes

The singular-value decomposition (SVD) of matrix $\mathbf{A} = [\mathbf{M}_1\ \mathbf{M}_2\ \mathbf{M}_3]$ confirms that the third deformation mode ($\mathbf{M}_3$) is in fact a linear combination of the first two modes (Figure 17).

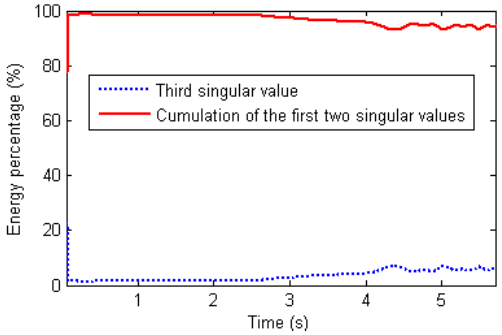

Figure 17 - Instantaneous singular values of the deformation mode matrix

In the following, the experiments were performed for 6 levels of excitation (L0-L5). The results of the WT in terms of instantaneous frequencies are given in Figure 18. Note that the distortions which appear in the evolution of the 2nd frequency were due to set-up problems and do not influence the detection procedure.

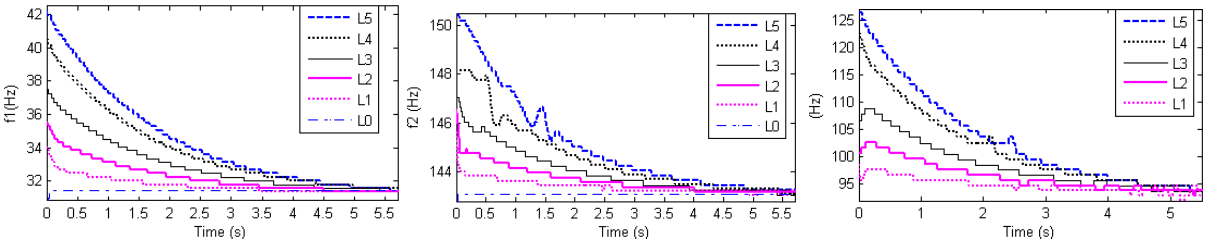

a) 1st ridge b) 2nd ridge c) 3rd ridge

Level	L5	L4	L3	L2	L1	L0
Max. displacement (mm)	1.37	1.20	0.93	0.72	0.48	0.037

Figure 18 - Instantaneous frequencies

Figure 19 gives the time evolution of subspace angles for the 6 levels of excitation. The angles are calculated respectively on the basis one single deformation mode ($\mathbf{M}_1$ or $\mathbf{M}_2$) in Figure 19 a)-b) and on the basis of the two independent 'modes' obtained through the SVD of the deformation mode matrix in Figure 19 c).

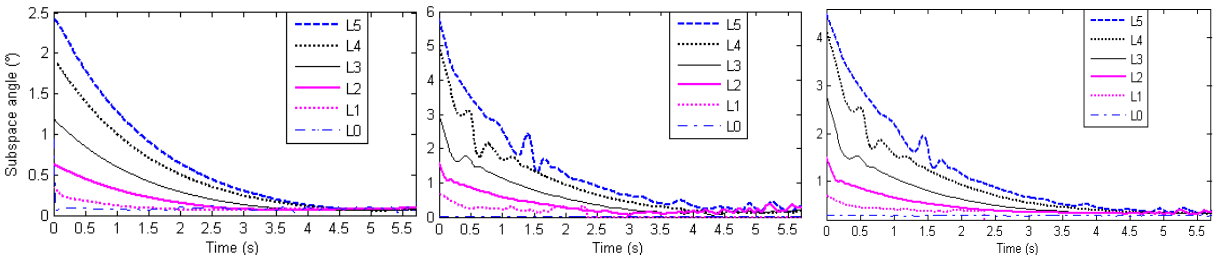

a) b) c)

Figure 19 - Time evolution of subspace angles for different excitation levels on the basis of 'mode' 1 (a), 'mode' 2 (b) and SVD modes (c)

Detection results are also given in Figure 20 in terms of displacement amplitude measured at the end of the beam at time t=0.125 *s*. In this figure, the first three points of the curves correspond to weak excitations (level L0). It can be seen how the magnitude of the nonlinearity depends on the displacement level. 'Mode' 2 looks more sensible to the nonlinearity than 'mode 1'.

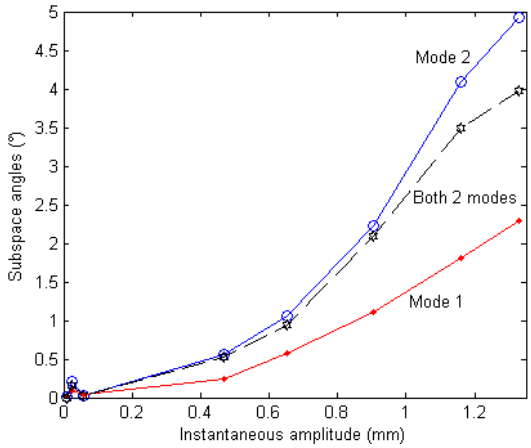

Figure 20 - Relation angles–displacement amplitudes at the end of beam, t = 0.125s

5. DISCUSSION AND COMPARISON WITH OTHER METHODS

Detection methods based on the measurement of instantaneous frequencies are reported by many authors in the literature. It was also achieved in this work as shown in Figures 11 and 18. Alternatively, deformation shapes provide important information about the change in the dynamics of a structure, which is very useful for detection purposes. The concept of subspace angle is an efficient tool that allows to quantitatively monitor the onset of damage or nonlinear behaviour through deformation modes. This was illustrated in Figures 12 and 19.

Through the above numerical and experimental examples, some remarks may be formulated on detection methods based on instantaneous features. We know that the time and frequency resolutions of the WT may be chosen e.g. to obtain a nice frequency resolution at a low frequency (e.g. ridge 1) but in this case, the resolution is much rougher at a high frequency (e.g. ridges 2, 3). In nonlinear systems, the presence of superharmonics of the first frequency has the effect of shortening the distance between this frequency component and ridge 1, ridge 2, etc. In order to avoid interferences between those ridges, it becomes necessary to increase the value of the central frequency ω_0 as required by the inequalities in (12). On the other hand, high frequencies (ridges 2, 3) can be identified with a satisfactory resolution by choosing a fine scale vector. However, a fine scale vector and a big value of ω_0 make the computation very costly. Although Figures 11, 18 have been achieved paying attention to the resolution, the results are not so smooth owing to the frequency resolution. Conversely, the detection indexes represented in Figures 12, 19 which are determined using the concept of subspace angle demonstrate quite smooth curves. It indicates the advantage of using instantaneous amplitudes: providing that an ω_0 high enough to well separate the ridges, the resolution is not a delicate problem for the instantaneous amplitude. It is illustrated in Appendix A by comparing the resolution in frequency and amplitude through a raw scale vector and a much finer one. In conclusion, the WT instantaneous amplitudes provide a good means of detection without the need to consider a sophisticated scale vector and the detection is advantageously performed through the use of the concept of subspace angle.

Other damage detection methods make use of the concept of subspace spanned by deformation modes as they are features of the dynamic system. For example, the subspace may be constructed (or identified) using experimental modal analysis (in the linear case), Principal Component Analysis (PCA) [4] or Null-Subspace Analysis - NSA [20]. Deformation modes can be also identified using Blind Source Separation (BSS) techniques such Independent Component Analysis (ICA) [5] or Second order Blind Identification (SOBI) [21]. The methods mentioned above are well established and may be used for modal identification but also for damage detection. However, those methods are appropriate for stationary signals and (mostly) linear systems. A unique set of mode shapes or principal components (PCs) do not allow to interpret the modulation of the dynamic behaviour during a vibration period in the case of non-stationary signals.

Another approach which is also known for its ability to analyze non-stationary signals is the Hilbert-Huang transform (HHT) [6-8]. The aim of the HHT method is to decompose a signal into instantaneous frequencies and intrinsic mode functions (IMFs). The IMFs which represent simple oscillatory modes could also be used for detection purposes in combination with the concept of subspace angle as proposed previously with the Wavelet Transform. However, the empirical framework of HHT still remains a drawback as it is based on numerical techniques such as approximation, optimization, etc.

6. CONCLUSION

The Wavelet Transform is known for its ability to analyze non-stationary signals and to detect nonlinear behaviour in a structure. As reported in [13], it can be used to identify instantaneous frequencies.

In this paper, detection of nonlinearity in a dynamic system submitted to impact excitation was performed using the concept of subspace angles between instantaneous deformation modes. These deformation modes are associated to instantaneous frequencies obtained from the wavelet transform of vibration signals measured at different coordinates of the system. Instantaneous bases of independent modes may be generated using the singular value decomposition of deformation mode matrices, which determines the dimensionality of the system.

The concept of subspace angles allows to define a global detection index. When used in combination with instantaneous modes extracted from the Wavelet Transform, this index was found to be sensitive to small dynamic changes and robust with regards to frequency resolution of the transform. The procedure was illustrated both numerically and experimentally on the example of a nonlinear cantilever beam.

ACKNOWLEDGEMENTS

The first author would like to thank Prof. P. Argoul and B. Godard for their help in the use of the WT.

7. REFERENCES

[1] Friswell M.I., Mottershead J.E., Ahmadian H., “Finite-element model updating using experimental test data: parametrization and regularization”, Transactions of the Royal Society of London, Series A, Special Issue on Experimental Modal Analysis, 359(1778), January 2001, pp.169-186.

[2] Titurus B., Friswell M.I., Starek L., “Damage detection using generic elements. Part I. Model updating”, Computers and Structures 81, 2003, pp.2273-2286.

[3] Titurus B., Friswell M.I., Starek L., “Damage detection using generic elements. Part II. Damage detection”, Computers and Structures 81, 2003, pp.2287-2299.

[4] De Boe P., Golinval J.C., “Principal component analysis of a piezosensor array for damage localization”, Structural Health Monitoring, 2003, pp.137-144.

[5] Zang C., Friswell M.I., Imregun M., “Structural damage detection using independent component analysis”, Structural Health Monitoring 3, 2004, pp.69-83.

[6] Huang N. et al. “The empirical mode decomposition and Hilbert spectrum for nonlinear and nonstationary time series analysis”. Pro. R. Soc. London (1998), Ser. A, 454, 903-995.

[7] Wu Z., Huang N.. “Ensemble empirical mode decomposition: a noise-assisted data analysis method”. Advances in Adaptive Data Analysis, Vol. 1, No.1 (2009), pp. 1-41.

[8] Yang J.N., Lei Y., Lin S., Huang N., “Hilbert – Huang based approach for structural damage detection”, Journal of Engineering Mechanics, No. 1, January 2004.

[9] Gurley K., Kareem A., “Applications of wavelet transforms in Earthquake, Wind and Ocean Engineering”, Engineering Structures 21, 1999, pp.149-167.

[10] Wang Weizhuo, Mottershead John E, Mares Cristinel, “Vibration mode shape recognition using image processing”, Journal of Sound and Vibration 326, pp. 909-938, 2009.

[11] Kijewski T., Kareem A., "Wavelet transforms for system identification in civil engineering", Computer-aided civil and Infrastructure Engineering 18, 2003, pp.339-355.
[12] Staszewski W. J., "Identification of non-linear systems using multi-scale ridges and skeletons of the Wavelet transform". Journal of Sound and Vibration (1998) 214 (4), pp.639-658.
[13] Argoul P. and Le T.-P., "Instantaneous indicators of structural behaviour based on the continuous Cauchy wavelet analysis", Mechanical Systems and Signal Processing 17(1), 2003, pp.243-250.
[14] Le T.-P., Argoul P., "Continuous wavelet transform for modal identification using free decay response", Journal of Sound and Vibration 277, Issues 1-2, 6 October 2004, pp.73-100.
[15] Erlicher S., Argoul P., "Modal identification of linear non-proportionally damped systems by wavelet transform", Mechanical Systems and Signal Processing 21, April 2007, pp.1386-1421.
[16] Mallat, "A wavelet tour of signal processing". Academic press, 1999.
[17] Golub G.H., Van Loan C.F., "Matrix computations" (3rd ed.), Baltimore, TheJohns Hopkins University Press, 1996.
[18] Lenaerts V., Kerschen G., Golinval J.C., "Proper Orthogonal Decomposition for Model Updating of Non-linear Mechanical Systems", Journal of Mechanical Systems and Signal Processing, 15(1), pp.31-43, 2001.
[19] Peeters M., Viguié R., Sérandour G., Kerschen G., Golinval J.C., "Nonlinear Normal Modes, Part II: Practical Computation using Numerical Continuation Techniques". Proceedings of the International Modal Analysis Conference, 2008.
[20] Yan A.M., Golinval J.C., "Null subspace-based damage detection of structures using vibration measurements", Mechanical Systems and Signal Processing 20, pp. 611-626, 2006.
[21] Poncelet F., Kerschen G., Golinval J.-C., Verhelst D., "Output-only modal analysis using blind source separation techniques", Mechanical Systems and Signal Processing 21, pp. 2335-2358, 2007.
[22] Jolliffe I.T., "Principal Component Analysis", Springer, Berlin, 1986.

APPENDIX A. Examples on the resolution of instantaneous frequency and amplitudes of the WT

Figure 21 shows identification results of ridge 2 using the WT of the signal measured at DOF 4 of the beam. In order to improve the resolution of the instantaneous frequency shown in Figure 21a, the scale vector was divided by five times to obtain the results presented in Figure 21b. It is observed that, although the instantaneous frequency is now better modulated, the instantaneous amplitude remains the same.

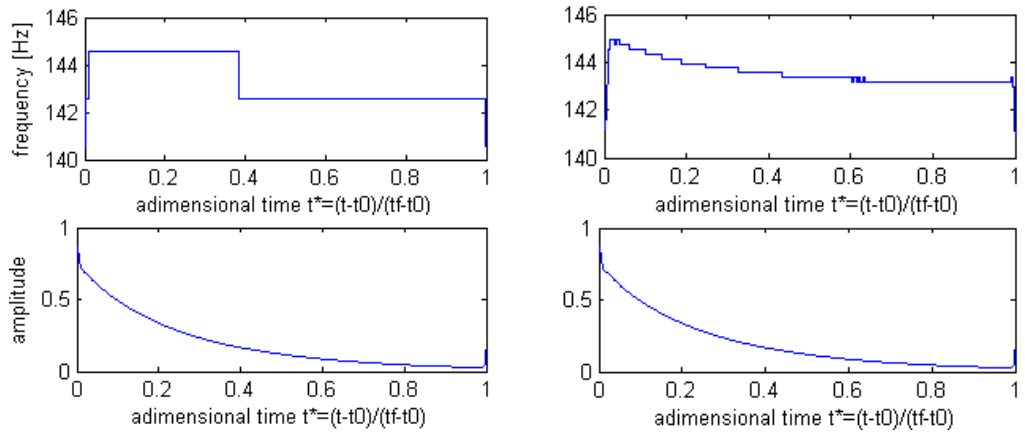

a) by a raw scale vector b) by a fine scale vector

Figure 21. Instantaneous frequency and amplitude using a raw scale vector (left) and a much finer scale vector (right)